Au_{34}^-: A Fluxional Core−Shell Cluster

Xiao Gu,[†] Satya Bulusu,[‡] Xi Li,[§,||] X. C. Zeng,[*,‡] Jun Li,[*,⊥] X. G. Gong,[*,†] and Lai-Sheng Wang[*,§,||]

Surface Physics Laboratory and Department of Physics, Fudan University, Shanghai 200433, China, Department of Chemistry and Center for Materials and Nanoscience, University of Nebraska, Lincoln, Nebraska 68588, Department of Physics, Washington State University, 2710 University Drive, Richland, Washington 99354, Chemical & Materials Sciences Division, Pacific Northwest National Laboratory, MS K8-88, P. O. Box 999, Richland, Washington 99352, and W. R. Wiley Environmental Molecular Sciences Laboratory, Pacific Northwest National Laboratory, MS K1-96, P. O. Box 999, Richland, Washington 99352

Received: March 10, 2007; In Final Form: April 10, 2007

Among the large Au_n^- clusters for $n > 20$, the photoelectron spectra of Au_{34}^- exhibit the largest energy gap (0.94 eV) with well-resolved spectral features, making it a good candidate for structural consideration in conjunction with theoretical studies. Extensive structural searches at several levels of density functional and ab initio theory revealed that the low-lying isomers of Au_{34}^- can be characterized as fluxional core−shell type structures with 4 or 3 inner atoms and 30 or 31 outer atoms, i.e., $Au_4@Au_{30}^-$ and $Au_3@Au_{31}^-$, respectively. Detailed comparisons between theoretical and photoelectron results suggest that the most probable ground state structures of Au_{34}^- are of the $Au_4@Au_{30}^-$ type. The 30 outer atoms seem to be disordered or fluxional, giving rise to a number of low-lying isomers with very close energies and simulated photoelectron spectra. The fluxional nature of the outer layer in large gold clusters or nanoparticles may have important implications for their remarkable catalytic activities.

Introduction

Although bulk gold is the most inert metal, gold nanoparticles have been found to display remarkable catalytic activities,[1] which has stimulated a resurgence of interest into the structures and properties of free gold nanoclusters. A detailed understanding at the atomic level of the structure−function relationship of well-defined gold clusters may hold the key to elucidate the catalytic mechanisms of nanogold. Anionic gold clusters are of particular interest because the extra electron seems to play an important role in activating molecules adsorbed on gold clusters and surfaces.

Anionic Au_n^- clusters with n up to 25 atoms have been characterized by a number of combined experimental and theoretical studies, showing a remarkable structural diversity. Small Au_n^- clusters have been discovered to be planar up to 12 gold atoms with the 2D to 3D transition occurring for $n > 12$.[2−4] In mid-sized gold clusters, Au_{20} has been found to be a perfect tetrahedron.[5] In a recent study, the structures of Au_n^- clusters in the size range of $n = 15-19$ were elucidated,[6] in which clusters with $n = 16-18$ were found to possess unprecedented empty cage structures, which have been confirmed by new experimental and theoretical studies[7−10] and endohedral doping.[11] In several very recent studies,[7,8,12] Au_n^- clusters beyond $n = 20$ have been characterized, all revealing complex potential energy surfaces with population of many low-lying isomers: the tetrahedral Au_{20}-based structures are competitive for $n = 21-23$, whereas a hollow tubular type structure appears for Au_{24}^-. Au_{25}^- possesses a core−shell type structure with a single internal atom.[12]

In larger systems, although Au_{32} was first suggested to be a "24-carat golden fullerene",[13,14] subsequent experiment showed that the Au_{32}^- anion is in fact a low-symmetry compact 3D structure,[15] which can also be viewed as a core−shell-type structure with three core atoms. There are no experimental characterizations of the structures for larger Au_n^- clusters, despite numerous theoretical efforts using both DFT-based methods and empirical potentials.[16−25]

First-principle global minimum searches for larger Au_n^- clusters are becoming a real challenge computationally. We have noted that among the large gold clusters the photoelectron spectra of Au_{34}^- display a considerable energy gap with well-resolved spectral features,[26,27] thus providing a unique opportunity for a joint experimental and theoretical effort to elucidate its structures. Photoelectron spectroscopy (PES) yields direct electronic structure information for the underlying clusters. Combined with accurate theoretical calculations, PES has become a powerful method to yield indirect structural information.

In this work, we report a joint PES and theoretical studies of Au_{34}^-. Extensive structural searches at several levels of theory revealed that the low-lying isomers of Au_{34}^- can be characterized as fluxional core−shell type structures with 4 or 3 inner atoms and 30 or 31 outer atoms, i.e., $Au_4@Au_{30}^-$ or $Au_3@Au_{31}^-$, respectively. Detailed comparisons between the theoretical and experimental results suggest that the most probable global minimum structures of Au_{34}^- are of the $Au_4@Au_{30}^-$ type. The 30 outer atoms seem to be disordered or fluxional, giving rise

* Corresponding authors. E-mail: ls.wang@pnl.gov (L.-S.W.); xczeng@phase2.unl.edu (X.C.Z.); xggong@fugan.edu.cn (W.G.G.); jun.li@pnl.gov (J.L.).
† Fudan University.
‡ University of Nebraska.
§ Washington State University.
|| Chemical & Materials Sciences Division, Pacific Northwest National Laboratory.
⊥ W. R. Wiley Environmental Molecular Sciences Laboratory, Pacific Northwest National Laboratory.

10.1021/jp071960b CCC: $37.00
Published on Web 05/17/2007

to a number of low-lying isomers with very close energies and simulated photoelectron spectra. The fluxional nature of the outer layer in large gold clusters or nanoparticles may have important implications for their remarkable catalytic activities.

Experimental Methods

The experiment was performed on a magnetic-bottle PES apparatus equipped with a laser vaporization supersonic cluster source.[28] The Au_{34}^- clusters were produced by laser vaporization of a pure gold disk target. Negatively charged clusters were extracted from the cluster beam and were analyzed using a time-of-flight mass spectrometer.[28] The Au_{34}^- clusters were mass selected and decelerated before being intercepted by a 193 nm laser beam from an ArF excimer laser or 266 nm from a Nd:YAG laser for photodetachment. Photoelectron time-of-flight spectra were calibrated using the known spectra of Au^- and converted to the binding energy spectra by subtracting the kinetic energy spectra from the photon energies. The resolution of the magnetic-bottle PES spectrometer was $\Delta E/E \sim 2.5\%$, i.e., about 25 meV for 1 eV electrons.

Computational Methods

We performed extensive searches for the low-lying isomers of Au_{34}^- using density functional methods implemented in VASP[29] and ADF,[30] and using basin-hopping methods.[31] We conducted our initial search for the possible structures of Au_{34}^- based on the local density approximation (LDA) using VASP, followed by geometry optimizations using generalized gradient approach (GGA) implemented in ADF. More than 20 structures were considered using these methods. In the VASP calculations, the $5d^{10}6s^1$ valence electrons were treated explicitly with scalar relativistic effects included, and their interactions with the ionic cores are described by the PAW potentials.[32] The Kohn−Sham orbitals were expanded in plane waves with an energy cutoff of ~230 eV. We used a simple cubic cell of edge length of 30 Å with periodic boundary conditions, and the Γ point approximation for the Brillouin zone sampling. The ADF calculations were performed using GGA of Perdew−Wang 1991 (PW91)[33] and Slater basis sets with quality of triple-ζ plus p- and f-polarization functions (TZ2P) for the valence orbitals of the Au atoms.[34] The frozen core approximation was applied to the $[1s^2\text{-}4f^{14}]$ core, with the $5s^25p^65d^{10}6s^1$ electrons explicitly treated variationally.[35] The scalar and spin−orbit relativistic effects were taken into account through zero-order-regular approach (ZORA).[36] Harmonic frequencies of the low-lying isomers were calculated using the PW91 functional to ensure the optimized structures were local minima.

We then performed a more exhaustive structural search using the basin-hopping approach, which sampled more than 50 structures. The basin-hopping search was directly combined with DFT calculations;[6,9,37] that is, after each accepted move, a geometry minimization was carried out using a DFT method. In the basin-hopping method, we used the gradient-corrected Perdew−Burke−Enzerhof (PBE) exchange-correlation functional[38] as implemented in the DMol^3 code.[39]

Top low-lying isomers obtained from both basin-hopping and VASP/ADF calculations were collected. The structures of these low-lying isomers were reoptimized by using the PBE functional[38] and LANL2DZ basis set[40] implemented in the Gaussian 03 package.[41] Inasmuch as DFT calculations do not account for the dispersion interactions between gold atoms, we also performed single-point energy calculation using the ab initio wave function approach for the nine low-lying isomers to further determine the relative stabilities of these isomers. The calculations were performed using NWChem 4.5[42] at the level of the second-order Møller−Plesset perturbation (MP2) theory with spin-unrestricted Hartree−Forck reference (i.e., UHF-UMP2).[43] The Hay−Wadt effective core potential[40] and LANL2DZ basis set were used in the MP2 calculations and the optimized geometries from PBE/LANl2DZ calculations were employed.

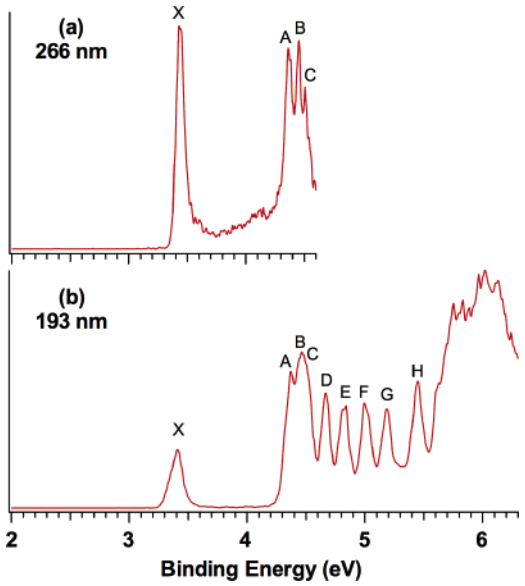

Figure 1. Photoelectron spectra of Au_{34}^- at (a) 266 nm (4.661 eV) and (b) 193 nm (6.424 eV).

Photoelectron spectra simulations were based on calculations using the PBE functional and LANL2DZ basis set. The first VDE was calculated from the energy difference between the anion and neutral clusters at the optimized anion geometry. VDEs to higher detachment channels were computed by adding to the first VDE the occupied orbital energies relative to the HOMO of Au_{34}^-. The simulated photoelectron spectra were obtained by fitting the computed VDE's with Gaussian functions of 0.04 eV width.

Experimental Results

Figure 1 presents the spectra of Au_{34}^- at two photon energies. The 266 nm spectrum exhibits an intense ground state band (X) followed by a large energy gap and three relatively sharp peaks (A, B, and C) at higher binding energies. The X band yields an adiabatic detachment energy or the electron affinity for neutral Au_{34} as 3.38 eV. At 193 nm, a series of well resolved bands (D−H) were observed between 4.5 and 5.5 eV followed by nearly continuous spectral features indicative of the onset of the 5d band.[26] The current spectrum at 193 nm is consistent with the previous study,[26] but with significantly improved resolution. The vertical detachment energies (VDE's) for all of the resolved spectral features are given in Table 1. The large X−A separation (0.94 eV) is consistent with the fact that the Au_{34} neutral cluster with 34 valence electrons represents a major spherical shell closing.[26] The weak electron signals in between the band gap in the 266 nm spectrum were most likely due to autodetachment, which was also observed in the 266 nm spectrum of the large band gap pyramidal Au_{20}^- cluster.[5]

Theoretical Results

A number of low-symmetry structures and some high-symmetry structures were obtained from the theoretical search for the optimal geometry of Au_{34}^-. The nine low-lying isomers obtained from basin-hopping and VASP/ADF calculations and

TABLE 1: Experimental Adiabatic (ADE) and Vertical (VDE) Detachment Energies of Au_{34}^- in eV

observed features	ADE	VDE
X	3.38 ± 0.04[a]	3.42 ± 0.03
A	4.32 ± 0.04	4.36 ± 0.03
B		4.45 ± 0.03
C		4.51 ± 0.03
D		4.67 ± 0.03
E		4.83 ± 0.03
F		5.00 ± 0.03
G		5.18 ± 0.03
H		5.45 ± 0.03

[a] The electron affinity of Au_{34}.

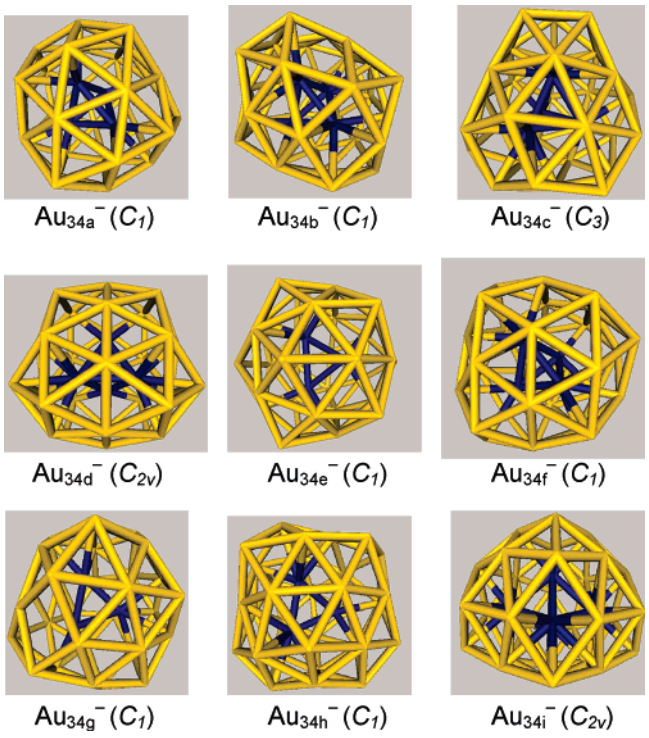

Figure 2. Optimized low-lying structures of Au_{34}^- at the PBE/LANL2DZ level of theory. See Table 2 for their energetic information.

TABLE 2: Optimized Low-Lying Structures for Au_{34}^-, Total Energies (E_{PBE}), Relative Energies (ΔE_{PBE}), and First Vertical Detachment Energies (VDE) at the PBEPBE/LANL2DZ Level of Theory[a]

structures	N_i	VDE (eV)	E_{PBE} (a.u.)	ΔE_{PBE} (eV)	ΔE_{MP2} (eV)
34a (C_1)	4	3.398	−4607.27944	0	0.000
34b (C_1)	4	3.440	−4607.27689	0.069	−0.047
34c (C_3)	4	3.538	−4607.27622	0.088	0.128
34d (C_{2v})	4	3.414	−4607.27432	0.139	−0.100
34e (C_1)	3	3.496	−4607.27385	0.152	1.120
34f (C_1)	4	3.415	−4607.27372	0.156	0.213
34g (C_1)	3	3.496	−4607.27124	0.223	1.624
34h (C_1)	3	3.470	−4607.26765	0.321	1.586
34i (C_{2v})	5	3.535	−4607.25155	0.759	3.117
experiment		3.42 ± 0.03			

[a] N_i represents the inner atoms in the core−shell structures.

geometry reoptimization with PBE/LANL2DZ are presented in Figure 2, and their total energies, relative energies, and calculated first VDEs are given in Table 2. The single-point MP2 energies are also listed in Table 2 for comparison. The simulated PES spectra from the nine low-lying isomers are shown in Figure 3.

All of the structures shown in Figure 2 are minima on the potential energy surface, and they can be viewed as containing a core with 3−5 atoms with a low-symmetry shell with 31−29 atoms. The inner core atoms are in blue color in Figure 2, and the number of core atoms is also given in Table 2 for each structure. In the VASP and ADF calculations, both isomer 34a and 34e are competing for the global minimum with very close energies, but in PBE/LANL2DZ, isomer 34e is 0.152 eV higher. Isomer 34c was the global minimum for neutral Au_{34} from the Sutton−Chen potential,[24] whereas isomer 34d was suggested to be the global minimum from a recent study using the Lennard-Jones potential followed by DFT optimization.[25] In an earlier VASP study, one of us (X.G.G.) showed that Au_{34} possesses a structure with an Au_{32} cage and two inner atoms.[14] Among the structures that we searched through DFT calculations, we found stable structures with empty cages and core−shell structures with 2−5 inner atoms. However, the most stable structures appear to contain 4 or 3 inner atoms with the $Au_4@Au_{30}^-$ structures being more favored, as shown in Figure 2. The MP2 energies of the nine low-lying isomers (Table 2) reveal that, among the two best candidate isomers for the global minimum with 4 and 3 inner atoms, 34a (−4579.60990 a.u.) is 1.12 eV lower than that of 34e (−4579.56875 a.u.). Furthermore, MP2 calculations indicate that all of the core−shell structures with 3 or 5 core atoms are much higher in energy than the isomers with 4 core atoms, whereas the structures with 4 core atoms lie close in energy, consistent with the fluxionality revealed from DFT calculations. These results suggest that the $Au_4@Au_{30}^-$ type structures are indeed favored and most likely to be the global minimum.

Discussion

The four lowest energy isomers (34a−d), which all contain 4 inner atoms, are competing for the global minimum. At both the PBE and MP2 levels of theory, these four isomers are nearly degenerate (Table 2). The first VDE for 34a,b,d are also nearly identical (~3.4 eV) with that of 34c being slightly higher (Table 2). Given the theoretical accuracy, the VDEs of the four lowest isomers are all in excellent agreement with the experimental value of 3.42 eV. Interestingly, the theoretical energy gaps for all of the four isomers are also similar and in good agreement with the experiment (Figure 3). However, the simulated spectra for the two higher symmetry isomers 34c (C_3) and 34d (C_{2v}) are relatively simple with fewer spectral features in the low binding energy range, seemingly inconsistent with the experimental spectra. The simulated spectra of both isomers 34a and 34b display similarities to the experimental PES spectra both in terms of the first calculated VDEs and the spectral patterns, although the simulated spectrum of isomer 34a shows the best overall agreement with the experiment. On the basis of the energetics, calculated VDEs, and the overall simulated spectral patterns, we conclude that isomer 34a is the most likely candidate responsible for the observed PES spectra with possible minor contributions from isomers 34b-d. However, all other isomers are more than 0.15 eV higher in energy and are not likely to make significant contributions to the experiment.

The shells of all of the low-lying core−shell isomers of Au_{34}^- shown in Figure 2 consist of 5- and 6-coordinated Au atoms. The top four isomers are all of the $Au_4@Au_{30}^-$ type (34a−d) with relatively small structural differences: the four core atoms form a slightly distorted tetrahedron and their main structural differences lie at the atomic connectivity of the 30 shell atoms. To gain further insight into the relationship between these structures, we carried out Car−Parrinello molecular dynamics

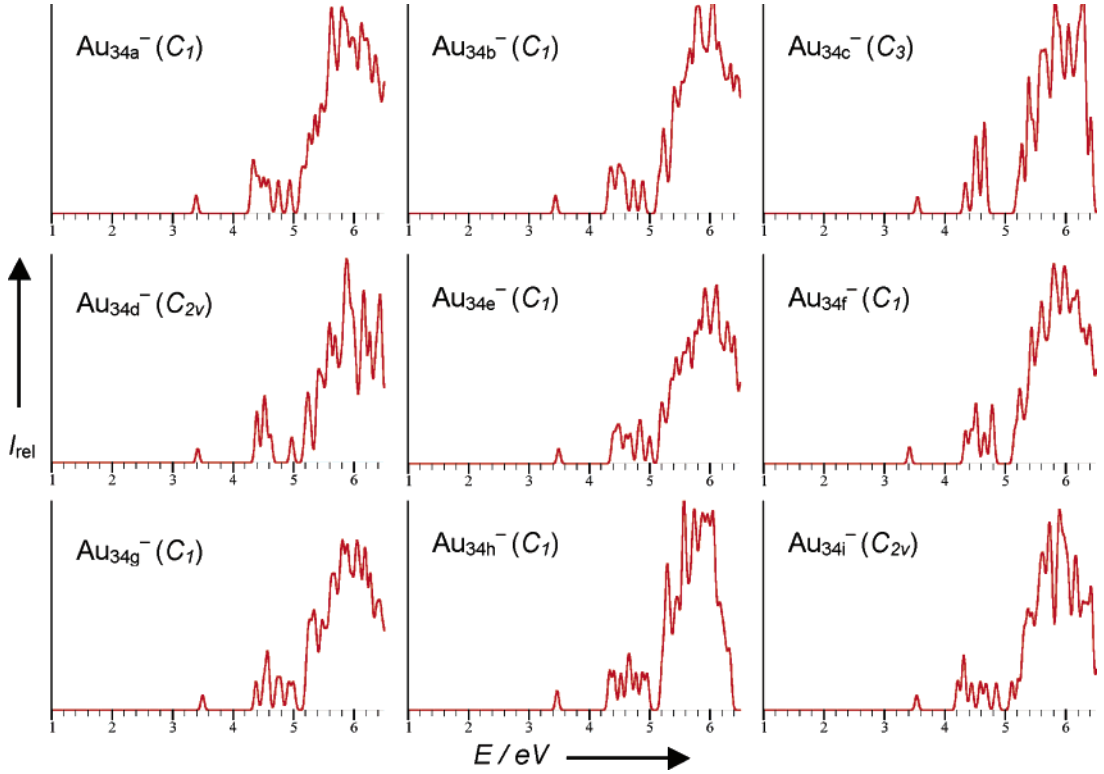

Figure 3. Simulated photoelectron spectra for the low-lying isomers of Au_{34}^-.

simulations.[44] We found that the shell is quite soft: the 5-coordinate atoms can easily rebond to a neighbor Au atom to form 6-coordinate ones, whereas some of the 6-coordinate atoms can be easily broken to 5-coordinate sites. However, during the simulations, the tetrahedral cores stay intact with only very slight distortions. These results suggest that in the gas-phase the Au_{34}^- cluster possesses a solid core with a somewhat fluctuating surface.

The fluctuating core−shell Au_{34}^- is consistent with previous studies that show that larger gold clusters tend to form amorphous structures.[16,17,18] A fluctuating surface in gold nanoclusters may have significant implications for understanding the catalytic mechanisms of gold nanoparticles. A fluctuating surface would guarantee the presence of low coordination surface sites, which are essential for chemisorption. The structural flexibility would also mean that the chemisorption energy of a single adsorbate may induce a structural change, which would benefit chemisorption of a second chemical reagent. We believe that continued and systematic understanding of the structural evolution of larger gold clusters may indeed provide key insight into their catalytic functions.

Note Added during Review. During the review of the present paper, a similar study on Au_{34}^- by Lechtken et al.[45] has appeared, which combines PES, trapped ion electron diffraction (TIED), and a limited theoretical search. In this study, two nearly degenerate low-lying isomers with C_3 and C_{2v} symmetries are identified, which coincide with the current isomers 34c and 34d, respectively. The simulated TIED of isomer 34c (C_3) agrees best with the experimental data, whereas that of 34d (C_{2v}) is also within the error limit and cannot be completely ruled out. The work by Lechtken et al. further points out nicely that the C_3 Au_{34}^- is a chiral gold cluster. The main conclusions of the work by Lechtken et al. are then consistent with the current work, although the lower symmetry isomers 34a and 34b are not considered.

Acknowledgment. X.G.G. is partially supported by the NSF of China, the Special Funds for Major National Basic Research, and Shanghai local government. He especially thanks E. Tosatti for helpful discussions. The experimental work done at Washington was supported by the U.S. NSF (CHE-0349426) and the John Simon Guggenheim Foundation and performed at the EMSL, a national scientific user facility sponsored by the U.S. DOE's Office of Biological and Environmental Research and located at PNNL, operated for DOE by Battelle. The theoretical work done at Nebraska was supported by the DOE Office of Basic Energy Sciences (DE-FG02-04ER46164), the NSF (CHE-0427746, CHE-0314577, and DMI-0210850), the John Simon Guggenheim Foundation, and the University of Nebraska—Lincoln Research Computing Facility. Part of the calculations was performed on the supercomputers at the EMSL Molecular Science Computing Facility, the Shanghai Supercomputer Center, and the Fudan Supercomputer Center.

References and Notes

(1) Haruta, M. *Catal. Today* **1997**, *36*, 153.
(2) Furche, F.; Ahlrichs, F.; Weis, P.; Jacob, C.; Gilb, S.; Bierweiler, T.; Kappes, M. M. *J. Chem. Phys.* **2002**, *117*, 6982.
(3) Häkkinen, H.; Moseler, M.; Landman, U. *Phys. Rev. Lett.* **2002**, *89*, 033401.
(4) Häkkinen, H.; Yoon, B.; Landman, U.; Li, X.; Zhai, H. J.; Wang, L. S. *J. Phys. Chem. A* **2003**, *107*, 6168.
(5) Li, J.; Li, X.; Zhai, H. J.; Wang, L. S. *Science* **2003**, *299*, 864.
(6) Bulusu, S.; Li, X.; Wang, L. S.; Zeng, X. C. *Proc. Natl. Acad. Sci. (U.S.A.)* **2006**, *103*, 8326.
(7) Xing, X. P.; Yoon, B.; Landman, U.; Parks, J. H. *Phys. Rev. B.* **2006**, *74*, 165423.
(8) Yoon, B.; Koskinen, P.; Huber, B.; Kostko, B.; Issendorff, B. v.; Häkkinen, H.; Moseler, M.; Landman, U. *ChemPhysChem.* **2007**, *8*, 157.
(9) Gao, Y.; Bulusu, S.; Zeng, X. C. *ChemPhysChem.* **2006**, *7*, 2275.
(10) Walter, M.; Häkkinen, H. *Phys. Chem. Chem. Phys.* **2006**, *8*, 5407.
(11) Wang, L. M.; Bulusu, S.; Zhai, H. J.; Zeng, X. C.; Wang, L. S. *Angew. Chem., Int. Ed.* **2007**, *46*, 2915.
(12) Bulusu, S.; Li, X.; Wang, L. S.; Zeng, X. C. *J. Phys. Chem. C* **2007**, *111*, 4190.

(13) Johansson, M. P.; Sundholm, D.; Vaara, J. *Angew. Chem., Int. Ed.* **2004**, *43*, 2678.
(14) Gu, X.; Ji, M.; Wei, S. H.; Gong, X. G. *Phys. Rev. B* **2004**, *70*, 205401.
(15) Ji, M.; Gu, X.; Li, X.; Gong, X. G.; Li, J.; Wang, L. S. *Angew. Chem. Int. Ed.* **2005**, *44*, 7119.
(16) Häkkinen, H.; Moseler, M.; Kostko, O.; Morgner, N.; Hoffmann, M. A.; Issendorff, B. v. *Phys. Rev. Lett.* **2004**, *93*, 093401.
(17) (a) Michaelian, M.; Rendon, N.; Garzón, I. L. *Phys. Rev. B* **1999**, *60*, 2000. (b) Garzón, I. L.; Michaelian, M.; Beltrán, M. R.; Posada-Amarillas, A.; Ordejón, P.; Artacho, E.; Sánchez-Portal, D.; Soler, J. M. *Eur. Phys. J. D* **1999**, *9*, 211.
(18) Lopez-Lozano, X.; Perez, L. A.; Garzón, I. L. *Phys. Rev. Lett.* **2006**, *97*, 233401.
(19) Gao, Y.; Zeng, X. C. *J. Am. Chem. Soc*. **2005**, *127*, 3698.
(20) Wang, J.; Jellinek, J.; Zhao, J.; Chen, Z.; King, R. B.; Schleyer, P. v. R. *J. Phys. Chem. A* **2005**, *109*, 9265.
(21) Häberlen, O. D.; Chung, S. C.; Stener, M.; Rösch, N. *J. Chem. Phys*. **1997**, *106*, 5189.
(22) Xiao, L.; Tollberg, B.; Hu, X. K.; Wang, L. C. *J. Chem. Phys*. **2006**, *124*, 114309.
(23) (a) Fa, W.; Dong, J. M. *J. Chem. Phys*. **2006**, *124*, 114310. (b) Fa, W.; Luo, C.; Dong, J. M. *Phys. Rev. B* **2005**, *72*, 205428.
(24) Doye, J. P. K.; Wales, D. J. *New J. Chem*. **1998**, *22*, 733.
(25) Bas, B. S. d.; Ford, M. J.; Cortie, M. B. *J. Mol. Struct.* (*THEOCHEM*) **2004**, *686*, 193.
(26) Taylor, K. J.; Pettiette-Hall, C. L.; Cheshnovsky, O.; Smalley, R. E. *J. Chem. Phys*. **1992**, *96*, 3319.
(27) Li, X.; Wang, L. S. unpublished results.
(28) Wang, L. S.; Cheng, H. S.; Fan, J. *J. Chem. Phys*. **1996**, *102*, 9480.
(29) Kresse, G.; Furthmüller, J. *Phys. Rev. B* **1996**, *54*, 11169.
(30) ADF 2005.01, SCM, Theoretical Chemistry; Vrije Universiteit: Amsterdam, The Netherlands (http://www.scm.com). (a) te Velde, G.; Bickelhaupt, F. M.; van Gisbergen, S. J. A.; Fonseca Guerra, C.; Baerends, E. J.; Snijders, J. G.; Ziegler, T. *J. Comput. Chem*. **2001**, *22*, 931. (b) Fonseca Guerra, C.; Snijders, J. G.; te Velde, G.; Baerends, E. J. *Theor. Chem. Acc*. **1998**, *99*, 391.
(31) Wales, D. J.; Scheraga, H. A. *Science* **1999**, *258*, 1368.
(32) Kresse, G.; Joubert, D. *Phys. Rev. B* **1999**, *59*, 1758.
(33) (a) Perdew, J. P.; Wang, Y. *Phys. Rev. B* **1992**, *45*, 13244. (b) Perdew, J. P.; Chevary, J. A.; Vosko, S. H.; Jackson, K. A.; Pederson, M. R.; Singh, D. J.; Foilhais, C. *Phys. Rev. B* **1992**, *46*, 6671.
(34) van Lenthe, E.; Baerends, E. J. *J. Comp. Chem.* **2003**, *24*, 1142.
(35) Baerends, E. J.; Ellis, D. E.; Ros, P. *Chem. Phys*. **1973**, *2*, 42.
(36) van Lenthe, E.; Baerends, E. J.; Snijders, J. G. *J. Chem. Phys*. **1993**, *99*, 4597.
(37) Yoo, S.; Zeng, X. C. *Angew. Chem. Int. Ed*. **2005**, *44*, 1491.
(38) Perdew, J. P.; Burke, K.; Enzerhof, M. *Phys. Rev. Lett*. **1996**, *77*, 3865.
(39) Delley, B. *J. Chem. Phys*. **1990**, *92*, 508.
(40) Hay, P. J.; Wadt, W. R. *J. Chem. Phys*. **1985**, *82*, 299.
(41) Frisch, M. J.; Trucks, G. W.; Schlegel, H. B.; Scuseria, G. E.; Robb, M. A.; Cheeseman, J. R.; Montgomery, J. A., Jr.; Vreven, T.; Kudin, K. N.; Burant, J. C.; Millam, J. M.; Iyengar, S. S.; Tomasi, J.; Barone, V.; Mennucci, B.; Cossi, M.; Scalmani, G.; Rega, N.; Petersson, G. A.; Nakatsuji, H.; Hada, M.; Ehara, M.; Toyota, K.; Fukuda, R.; Hasegawa, J.; Ishida, M.; Nakajima, T.; Honda, Y.; Kitao, O.; Nakai, H.; Klene, M.; Li, X.; Knox, J. E.; Hratchian, H. P.; Cross, J. B.; Bakken, V.; Adamo, C.; Jaramillo, J.; Gomperts, R.; Stratmann, R. E.; Yazyev, O.; Austin, A. J.; Cammi, R.; Pomelli, C.; Ochterski, J. W.; Ayala, P. Y.; Morokuma, K.; Voth, G. A.; Salvador, P.; Dannenberg, J. J.; Zakrzewski, V. G.; Dapprich, S.; Daniels, A. D.; Strain, M. C.; Farkas, O.; Malick, D. K.; Rabuck, A. D.; Raghavachari, K.; Foresman, J. B.; Ortiz, J. V.; Cui, Q.; Baboul, A. G.; Clifford, S.; Cioslowski, J.; Stefanov, B. B.; Liu, G.; Liashenko, A.; Piskorz, P.; Komaromi, I.; Martin, R. L.; Fox, D. J.; Keith, T.; Al-Laham, M. A.; Peng, C. Y.; Nanayakkara, A.; Challacombe, M.; Gill, P. M. W.; Johnson, B.; Chen, W.; Wong, M. W.; Gonzalez, C.; Pople, J. A. *Gaussian 03*, revision C.02; Gaussian, Inc.: Wallingford, CT, 2004.
(42) Straatsma, T. P.; Apra, E.; Windus, T. L.; Dupuis, M.; Bylaska, E. J.; de Jong, W.; Hirata, S.; Smith, D. M. A.; Hackler, M. T.; Pollack, L.; Harrison, R. J.; Nieplocha, J.; Tipparaju, V.; Krishnan, M.; Brown, E.; Cisneros, G.; Fann, G. I.; Fruchtl, H.; Garza, J.; Hirao, K.; Kendall, R.; Nichols, J. A.; Tsemekhman, K.; Valiev, M.; Wolinski, K.; Anchell, J.; Bernholdt, D.; Borowski, P.; Clark, T.; Clerc, D.; Dachsel, H.; Deegan, M.; Dyall, K.; Elwood, D.; Glendening, E.; Gutowski, M.; Hess, A.; Jaffe, J.; Johnson, B.; Ju, J.; Kobayashi, R.; Kutteh, R.; Lin, Z.; Littlefield, R.; Long, X.; Meng, B.; Nakajima, T.; Niu, S.; Rosing, M.; Sandrone, G.; Stave, M.; Taylor, H.; Thomas, G.; van Lenthe, J.; Wong, A.; Zhang, Z. *NWChem, A Computational Chemistry Package for Parallel Computers*, version 4.5; Pacific Northwest National Laboratory: Richland, WA, 2003.
(43) Møller, C.; Plesset, M. S. *Phys. Rev*. **1934**, *46*, 618.
(44) Car, R.; Parrinello, M. *Phys. Rev. Lett*. **1985**, *55*, 2471.
(45) Lechtken, A.; Schoos, D.; Stairs, J. R.; Blom, M. N.; Furche, F.; Morgner, N.; Kostko, O.; Issendorff, B. v.; Kappes, M. M. *Angew. Chem. Int. Ed*. **2007**, *46*, 2944.